BIOCHEMISTRY
including biophysical chemistry & molecular biology

Article

pubs.acs.org/biochemistry

The Carboxyl Terminus of Eremomycin Facilitates Binding to the Non-D-Ala-D-Ala Segment of the Peptidoglycan Pentapeptide Stem

James Chang,[†] Hongyu Zhou,[‡] Maria Preobrazhenskaya,[§] Peng Tao,[‡] and Sung Joon Kim*[,†]

[†]Department of Chemistry and Biochemistry, Baylor University, Waco, Texas 76706, United States

[‡]Department of Chemistry, Center for Drug Discovery, Design, and Delivery (CD4), Center for Scientific Computation, Southern Methodist University, Dallas, Texas 75275, United States

[§]Gause Institute of New Antibiotics, Moscow, Russian Federation

Supporting Information

ABSTRACT: Glycopeptide antibiotics inhibit cell wall biosynthesis in Gram-positive bacteria by targeting the peptidoglycan (PG) pentapeptide stem structure (L-Ala-D-iso-Gln-L-Lys-D-Ala-D-Ala). Structures of the glycopeptide complexed with a PG stem mimic have shown that the D-Ala-D-Ala segment is the primary drug binding site; however, biochemical evidence suggests that the glycopeptide−PG interaction involves more than D-Ala-D-Ala binding. Interactions of the glycopeptide with the non-D-Ala-D-Ala segment of the PG stem were investigated using solid-state nuclear magnetic resonance (NMR). LCTA-1421, a double ^{15}N-enriched eremomycin derivative with a C-terminal [^{15}N]amide and [^{15}N]Asn amide, was complexed with whole cells of *Staphylococcus aureus* grown in a defined medium containing L-[3-^{13}C]Ala and D-[1-^{13}C]Ala in the presence of alanine racemase inhibitor alaphosphin. ^{13}C{^{15}N} and ^{15}N{^{13}C} rotational-echo double-resonance (REDOR) NMR measurements determined the ^{13}C−^{15}N internuclear distances between the [^{15}N]Asn amide of LCTA-1421 and the ^{13}C atoms of the bound D-[1-^{13}C]Ala-D-[1-^{13}C]Ala to be 5.1 and 4.8 Å, respectively. These measurements also determined the distance from the C-terminal [^{15}N]amide of LCTA-1421 to the L-[3-^{13}C]Ala of PG to be 3.5 Å. The measured REDOR distance constraints position the C-terminus of the glycopeptide in the proximity of the L-Ala of the PG, suggesting that the C-terminus of the glycopeptide interacts near the L-Ala segment of the PG stem. *In vivo* REDOR measurements provided structural insight into how C-terminally modified glycopeptide antibiotics operate.

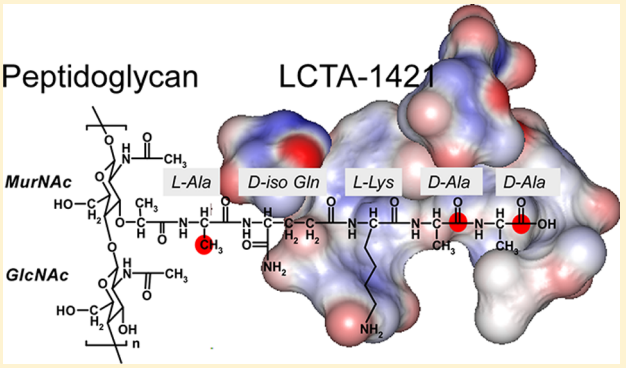

Vancomycin is a glycopeptide antibiotic exhibiting potent activities against almost all strains of Gram-positive cocci and bacilli.[1] In 1956, Eli Lilly and Company discovered vancomycin in soil samples collected from Borneo; the antibiotic was being produced by soil microbe *Amycolatopsis orientalis*. Since the discovery of vancomycin, researchers have identified ∼50 different glycopeptide antibiotic-producing organisms with more than 100 different natural glycopeptides.[2,3] All glycopeptides have a heptapeptide core (aglycon) structure formed by heavily cross-linked amino acids through a series of phenolic oxidative couplings. The glycopeptides are classified into four types on the basis of their chemical structure (Supplementary Figure S1).[4] Vancomycin is a Type I glycopeptide with methylated leucine and asparagine at the first and third positions of the aglycon, respectively. In Type II glycopeptides, such as avoparcin, the first and third residues are replaced by aromatic amino acids. Type III and IV glycopeptides also have aromatic amino acids at the first and third positions, but they are cross-linked by a phenolic−ether linkage. Ristocetin is an example of a Type III glycopeptide, with its aglycon structure modified by six sugar adducts. Teicoplanin, a Type IV glycopeptide, has an aglycon core structure identical to that of Type III but differs by an acyl chain attached to the sugar moiety.

Glycopeptides inhibit peptidoglycan (PG) biosynthesis by binding to lipid II, a membrane-bound PG precursor. This behavior was discovered when vancomycin was added to cell extracts of *Staphylococcus aureus* inhibited the formation of the PG (Figure 1) and the incorporation of glycine into lipid II.[5] When vancomycin is added to whole cells of bacteria, cytoplasmic precursors accumulate (Park's nucleotide) and the cell wall becomes thinner. These results support the hypothesis that vancomycin inhibits transglycosylation by targeting lipid II.[6] By binding to lipid II, vancomycin effectively sequesters the lipid transporter C_{55}, the limiting factor in PG biosynthesis, which is present only in a small number of copies per bacterium. The lipid transporter is regenerated from lipid II only during the transglycosylation step of PG biosynthesis.

Received: February 29, 2016
Revised: May 27, 2016
Published: May 31, 2016

DOI: 10.1021/acs.biochem.6b00188
Biochemistry 2016, 55, 3383−3391

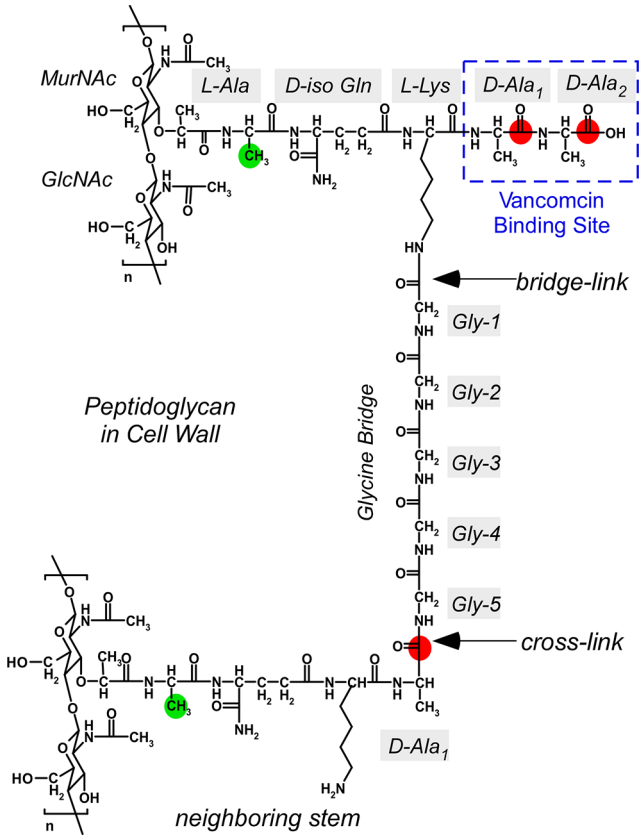

Figure 1. Chemical structure of *S. aureus* cell wall peptidoglycan (PG). PG has a repeat unit consisting of a disaccharide (MurNAc-GlcNAc) and a pentapeptide stem consisting of the sequence L-Ala-D-iso-Gln-L-Lys-D-Ala-D-Ala. A pentaglycine bridge is attached to the ϵ-nitrogen of the L-Lys. The ^{13}C isotope-enriched labels are incorporated into PG by growing *S. aureus* in the defined medium containing D-[1-^{13}C]Ala and L-[3-^{13}C]Ala, in the presence of the alanine racemase inhibitor alaphosphin (5 μg/mL). The positions of ^{13}C isotope-enriched labels for the D-[1-^{13}C]Ala are shown as red circles and those of L-[3-^{13}C]Ala as green circles. The dotted blue box indicates the D-Ala-D-Ala terminus of the PG stem, the known vancomycin binding site.

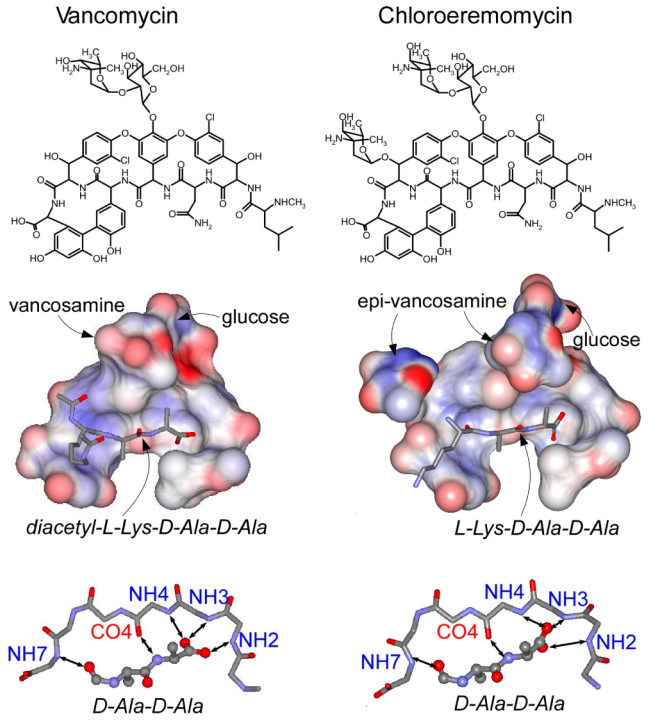

Figure 2. Chemical structures (top) of Type I glycopeptides, vancomycin (left) and chloroeremomycin (right). The heptapeptide core is heavily cross-linked and modified by sugars. The disaccharide of vancomycin is glucose-vancosamine, and the disaccharide of eremomycin is glucose-4-epi-vancosamine. An X-ray crystal structure (middle) of vancomycin (left) complexed with the diacetyl-L-Lys-D-Ala-D-Ala segment (PDB entry 1FVM)[42] and a solution-state NMR structure of chloroeremomycin (right) complexed with L-Ala-D-iso-Glu-L-Lys-D-Ala-D-Ala (PDB entry 1GAC).[10] The L-Ala-D-iso-Glu segment of the bound ligand has been omitted from the chloroeremomycin structure for the sake of clarity. PG stem binding (bottom) involves the formation of five hydrogen bonds connecting the heptapeptide backbone structures of vancomycin (left) and chloroeremomycin (right) to the dipeptide D-Ala-D-Ala. The glycopeptide backbones are labeled by the residue numbers, and the hydrogen bonds are represented as arrows. The side chains of glycopeptides and the D-Ala-D-Ala frawent have been omitted for the sake of clarity.

Binding of vancomycin to D-Ala-D-Ala was first identified when vancomycin failed to inhibit *in vitro* PG polymerization of UDP-MurNac-tetrapeptide purified from the membrane fractions of *Gaffkya homari*.[7] Because the UDP-MurNac-tetrapeptide lacked the terminal D-Ala found on the PG-pentapeptide stem (Figure 1), it was inferred that vancomycin operates in part by binding to the terminal D-Ala-D-Ala of PG. When the addition of the D-Ala-D-Ala dipeptide antagonized vancomycin's activities, this finding confirmed that the D-Ala-D-Ala segment of PG is the vancomycin binding site. The vancomycin dissociation constant for acyl-D-Ala-D-Ala, determined by capillary electrophoresis, is 4.3 μM.[8]

Figure 2 shows the X-ray crystal structure of vancomycin bound to diacetyl-L-Lys-D-Ala-D-Ala[9] and the solution-state NMR structure of chloroeremomycin complexed with PG precursor analogue L-Ala-D-iso-Glu-L-Lys-D-Ala-D-Ala.[10] Both vancomycin and chloroeremomycin share an identical heptapeptide core structure that forms the D-Ala-D-Ala binding site. Five hydrogen bonds stabilize the D-Ala-D-Ala segment as it is attached to the aglycon structure (Figure 2, bottom). (i) The first three H-bonds are located between the amide protons (NH2−NH4) and the carboxyl oxygen on the C-terminus of the D-Ala-D-Ala segment. (ii) A fourth bond is located between the carbonyl oxygen on the fourth residue of the aglycon (CO4) and an amide proton of the terminal D-Ala. (iii) A fifth bond is located between the amide proton of the seventh residue of the aglycon (NH7) and the carbonyl oxygen of the L-Lys. The hydrophobic interactions between the aromatic residues of the glycopeptide core structure and the methyl group of the alanines in the dipeptide are thought to further stabilize the drug-bound structure. In both X-ray crystal and solution-state NMR structures, the disaccharides of vancomycin and chloroeremomycin do not participate in D-Ala-D-Ala binding.

Structure and activity studies of glycopeptides and biochemical evidence suggest that *in vivo* glycopeptide−PG binding is far more complex than mere D-Ala-D-Ala dipeptide binding.[2,11] Some of the evidence is listed here. (1) The strength of the glycopeptide's binding affinity for D-Ala-D-Ala does not correlate with the drug's activity. For example, the binding affinity between chloroeremomycin and diacetyl-L-Lys-D-Ala-D-Ala is approximately 23 times lower than that of vancomycin, but its activity is approximately 5−10 times

DOI: 10.1021/acs.biochem.6b00188
Biochemistry 2016, 55, 3383−3391

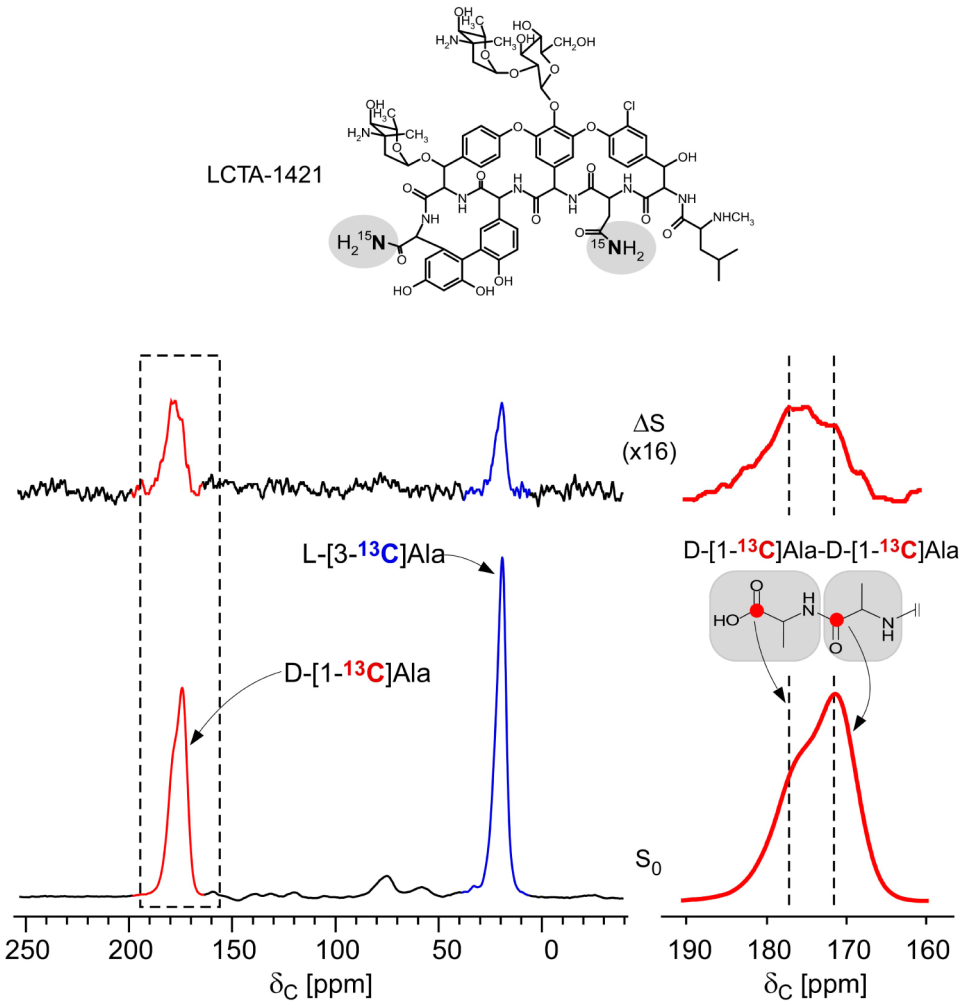

Figure 3. Chemical structure of LCTA-1421 (top). LCTA-1421 has two ^{15}N isotope-enriched labels (gray circles). The first is a C-terminal [^{15}N]amide and the second a [^{15}N]amide side chain of an asparagine. LCTA-1421 shows improved antimicrobial activity. Supplementary Table S2 summarizes the minimum inhibitory concentrations of vancomycin, eremomycin, and C-terminally modified eremomycins against vancomycin sensitive and vancomycin-resistant strains. $^{13}C\{^{15}N\}$ REDOR spectra (bottom) during the 32.4 ms dipolar evolution of whole cells of *S. aureus* grown in defined medium containing D-[1-^{13}C]Ala and L-[3-^{13}C]Ala complexed to LCTA-1421. In the left panel, the alanyl-carbonyl carbon of D-[1-^{13}C]Ala is visible at 175 ppm (red) and the alanyl-methyl carbon of L-[3-^{13}C]Ala is visible at 30 ppm (blue) in the reference spectra (bottom). In the difference ΔS spectra (top), only the carbons that are in dipolar contact with the ^{15}N of LCTA-1421 are visible. Both the alanyl-carbonyl carbon of D-[1-^{13}C]Ala at 175 ppm (red) and the alanyl-methyl carbon of L-[3-^{13}C]Ala at 30 ppm (blue) are dephased by the ^{15}N of LCTA-1421. In the right panel, the carbons of D-[1-^{13}C]Ala are resolved. The spectra were the result of the accumulation of 160000 scans.

greater. (2) The chlorine atom on the second amino acid of vancomycin improves the activity. The dechlorinated vancomycin (monodechlorovancomycin) is only half as active as vancomycin. (3) The removal of sugars from vancomcyin (deglycosylated vancomycin) does not affect D-Ala-D-Ala binding, but it reduces the activity by a factor of 5. The sugars on vancomycin have been attributed to the formation of a drug dimer, but *in vivo* glycopeptides are found as monomers,[12−16] which suggests that the sugars enhance the activity by facilitating PG binding through sugar−PG interactions.[15] (4) Methylated leucine, the first amino acid on vancomycin, is crucial for activity. The Edman degradation removal of leucine destroys the dipeptide binding affinity and its activity. (5) Asparagine, the third residue of vancomycin, does not participate in D-Ala-D-Ala binding but is required for its activity.[17] Replacing asparagine with glutamine (lengthening the side chain by one carbon) or replacing it with an aspartate (introducing negative charge) reduces the activity by 2- and 10-fold, respectively. Substitution of asparagine with isoasparte destroys the antimicrobial activity.[2,11] (6) Alkylation of the drug sugar by a hydrophobic side chain improves the activity.[18−21] (7) The carboxyl-terminal modifications of the glycopeptide improve the activity even though it is not involved in D-Ala-D-Ala binding.[22]

In this study, we investigate *in vivo* glycopeptide−PG binding interactions using solid-state NMR. Unlike solution-state NMR and X-ray diffraction structures based on the drug bound to PG-mimicking peptides, solid-state NMR allows direct investigation of the glycopeptide−PG complex in intact whole cells of *S. aureus*. To probe the glycopeptide−PG interactions, we have synthesized eremomycin derivative LCTA-1421 (Figure 3, top). LCTA-1421 is a bis[^{15}N]amide-carboxyeremomycin with two ^{15}N isotope-labeled probes: (1) a [^{15}N]amide at the asparagine side chain of the aglycon structure positioned inside the D-Ala-D-Ala binding pocket and (2) a C-terminal [^{15}N]amide at the seventh amino acid position.

The first probe, [^{15}N]amide asparagine of LCTA-1421, was used to characterize the structure of the LCTA-1421 aglycon

DOI: 10.1021/acs.biochem.6b00188
Biochemistry 2016, 55, 3383−3391

bound to the D-Ala-D-Ala segment of the PG stem in whole cells. We anticipated that the *in situ* aglycon structure of LCTA-1421 bound to the D-Ala-D-Ala segment of PG in the cell wall will be different from the solution-state NMR and X-ray diffraction structures based on the drug bound to a model peptide that suffers from the artifacts of drug dimerization and crystal lattice constraints, respectively. The *in situ* aglycon structure of LCTA-1421 bound to PG was inferred from the internuclear $^{13}C-^{15}N$ distance measurements between the Asn [^{15}N]amide of LCTA-1421 and the ^{13}C atoms in D-[1-^{13}C]Ala-D-[1-^{13}C]Ala of the PG stem using rotational-echo double-resonance (REDOR) NMR.[23,24]

The second probe, the C-terminal [^{15}N]amide of LCTA-1421, was used to determine whether interaction of the glycopeptide with the non-D-Ala-D-Ala segment of the PG stem structure by measuring the $^{13}C-^{15}N$ distance between the C-terminal [^{15}N]amide of LCTA-1421 and the ^{13}C in L-[3-^{13}C]Ala of the PG stem. LCTA-1421 exhibits improved antimicrobial activity versus that of the parent compound (Supplementary Table S2), which suggests that the interaction of the C-terminal [^{15}N]amide of LCTA-1421 with the non-D-Ala-D-Ala segment of PG stem is important for enhancing antimicrobial activity. Thus, further understanding the interactions of the glycopeptide with the non-D-Ala-D-Ala segment of the PG stem is crucial for the future development of novel therapeutic agents, in particular against the vancomycin-resistant enterococci whose mechanism of vancomycin resistance is based on modification of the D-Ala-D-Ala segment of the PG stem to D-Ala-D-Lac.

MATERIALS AND METHODS

Synthesis of LCTA-1421 and LCTA-1110. The synthesis of bis[^{15}N]amide-carboxyeremomycin (LCTA-1421) was described by Solov'eva et al.[25] Briefly, eremomycin was treated with barium hydroxide at 37 °C for 4 h to yield carboxyeremomycin.[17] [^{15}N]Ammonium chloride was used to incorporate ^{15}N-enriched labels at amino acid positions 3 and 7 of carboxyeremomycin using PyBOP and HBPyU as condensing reagents.[25] The MS-ESI-calculated mass for LCTA-1421 ($C_{73}H_{90}N_9{}^{15}N_2O_{25}Cl$, $[M + H]^+$) was 1557.57, and the found $[M + 2H]^{2+}$ mass was 779.80. The chemical shift of the [^{15}N]amide at the C-terminus (amino acid position 7) was 110.22 ppm, and the [^{15}N]amide side chain of asparagine (amino acid position 3) was 113.28 ppm as determined by solution-state NMR. The synthesis of eremomycin *p*-fluorophenylpiperazinamide (LCTA-1110) has been described elsewhere,[26] but briefly, LCTA-1110 was obtained by condensation of eremomycin with 4-fluorophenylpiperazine using PyBOP or HBPyU as a condensing reagent.

Minimum Inhibitory Concentrations of Glycopeptide Antibiotics. As recommended by the National Committee for Clinical Laboratory Standards, the microdilution method using Mueller-Hinton broth determined minimal inhibitory concentrations (MICs) for vancomycin, eremomycin, LCTA-1421, and LCTA-1110 against *Staphylococcus epidermidis*, *Staphylococcus hemolyticus*, vancomycin intermediate-resistant *S. aureus* (VISA), vancomycin-susceptible *Enterococcus faecium*, vancomycin-susceptible *Enterococcus faecalis*, vancomycin-resistant *E. faecium* (VanA type), and vancomycin-resistant *E. faecalis* (VanA type).

Growth of Whole Cells of *S. aureus*. A starter culture of *S. aureus* (ATCC 6538P) was added (1% final volume) to a 1 L flask containing 250 mL of sterile *S. aureus* standard medium (SASM), which consists of L-[3-^{13}C]Ala and D-[1-^{13}C]Ala in the presence of the alanine racemase inhibitor alaphosphin (5 mg/L). The detailed protocol for preparing SASM has been described elsewhere.[15,16,27] The cells were harvested at an optical density at 660 nm of 1.0, washed twice, and then resuspended in 10 mL of water containing 7.1 mg of LCTA-1421. After 10 min on ice, the LCTA-1421−bacterium complex was frozen using liquid N_2 and then lyophilized. The lyophilized sample weight was 250 mg.

Solid-State NMR Spectrometer and REDOR NMR Parameters. REDOR NMR experiments were performed on an 89 mm bore Oxford (Cambridge, England) superconducting solenoid at 4.7 T (200 MHz for ^1H), using a four-frequency transmission line probe with a Chemagnetics/Varian ceramic stator. The samples were contained in a 7.5 mm outside diameter zirconia rotor spinning at 5 kHz at room temperature. Radiofrequency pulses for ^{13}C and ^{15}N were produced by 1 kW ENI (Andover, MA) LPI-10 power amplifiers. Radiofrequency pulses for ^1H were produced by a 1 kW Kalmus Engineering Ltd. (Valencia, CA) power amplifier and the ^{19}F pulses by a 1 kW Dressler Hochfrequenztechnik Gmbh (Stolberg-Vicht, Germany) power amplifier. All four amplifiers were under active control. Radiofrequency pulse lengths for the π pulse were 10 μs for ^{13}C, ^{15}N, and ^{19}F. Proton−carbon and proton−nitrogen matched cross-polarization transfers were at 50 kHz for 2 ms. Proton dipolar decoupling during signal acquisition was 105 kHz. Standard XY-8 phase cycling[28] was used for all refocusing and dephasing pulses.

The REDOR NMR method recouples heteronuclear dipolar interactions under magic-angle spinning (MAS)[23,24] to determine heteronuclear dipolar couplings and hence internuclear distances. REDOR NMR has been described elsewhere;[15,16,27] briefly, in the full-echo (S_0) spectrum, dipolar dephasing is refocused over a single rotor period by MAS. In the S spectrum, the spin part of the dipolar interaction prevented full refocusing via application of dephasing π pulses, which reduced the peak intensity for dipolar coupled spin pairs. The difference in signal intensity ($\Delta S = S_0 - S$) for the observed spin (^{13}C or ^{15}N) is directly related to the heteronuclear dipolar coupling from which the corresponding distance to the dephasing spin is determined. The normalized REDOR difference ($\Delta S/S_0$), based on the peak height measurements, is a direct measure of dipolar coupling, which was calculated using the modified Bessel function expressions given by Mueller et al.[29] and de la Caillerie and Fretigny[30] for an IS spin-$^1/_2$ pair. The error bar for each REDOR dephasing was determined on the basis of the maximal noise peak intensity with respect to the dephased peak intensity.

Molecular Dynamics Simulation of the PG−LCTA-1421 Complex. Molecular dynamics simulation of LCTA-1421 bound to the PG pentapeptide stem structure was performed without water molecules to focus on the drug−target binding interactions. The initial model was generated on the basis of the NMR structure of chloroeremomycin complexed to the PG stem structure (L-Ala-D-iso-Gln-L-Lys-D-Ala-D-Ala) (PDB entry 1GAC). The CHARMM General Force Field (CGenFF)[31] for the simulating system was generated using the online server ParamChem (https://cgenff.paramchem.org/). After a 20 ns molecular dynamics simulation, the following distance constraints were applied: (i) 3.5 Å between L-[3-^{13}C]Ala and a [^{15}N]amide at the C-terminus of LCTA-1421, (ii) 5.1 Å between D-[1-^{13}C]Ala and the asparagine [^{15}N]amide in LCTA-1421, and (iii) 4.8 Å between

DOI: 10.1021/acs.biochem.6b00188
Biochemistry 2016, 55, 3383−3391

D-[1-^{13}C]Ala and the [^{15}N]amide at the C-terminus of LCTA-1421. Additional harmonic constraints (5 kcal/mol) were added to prevent the simulation from deviating from the NMR structure.

RESULTS

^{13}C{^{15}N}REDOR NMR of the PG–LCTA-1421 Complex. ^{13}C{^{15}N}REDOR spectra during 32.4 ms dipolar evolution for whole cells of *S. aureus* labeled with D-[1-^{13}C]Ala and L-[3-^{13}C]Ala complexed with LCTA-1421 are shown in Figure 3. For *S. aureus* grown in the presence of alaphosphin (5 μg/mL), the provisioned D-[1-^{13}C]Ala does not scramble to L-[1-^{13}C]Ala.[32] The ^{13}C carbonyl carbons of D-[1-^{13}C]Ala-D-[1-^{13}C]Ala appear at 175 ppm (red), and the ^{13}C methyl carbon of L-[3-^{13}C]Ala appears at 30 ppm (blue). The chemical shift assignments for the ^{13}C carbonyl carbons of D-[1-^{13}C]Ala-D-[1-^{13}C]Ala were determined using a ^{13}C → ^{15}N transferred-echo double-resonance NMR experiment with whole cells of *S. aureus* labeled with D-[1-^{13}C]Ala and [^{15}N]Gly.[33] In the difference (Δ*S*) spectrum, both 175 and 30 ppm peaks are dephased by the ^{15}N atoms of LCTA-1421. An expanded region centered around 175 ppm (right panel) shows that the ^{13}C carbonyl carbon of D-[1-^{13}C]Ala is partially resolved. The 178 ppm peak is assigned to the carboxyl carbonyl carbon and the 173 ppm peak to the peptidyl carbonyl carbon of the D-[1-^{13}C]Ala-D-[1-^{13}C]Ala segment in the PG stem.[33] The ^{13}C carbonyl carbons of D-[1-^{13}C]Ala-D-[1-^{13}C]Ala are dephased exclusively by the asparagine [^{15}N]amide of LCTA-142 because of its position found near the bound D-Ala-D-Ala segment.[9] The methyl carbon of L-[3-^{13}C]Ala, on the other hand, is exclusively dephased by the C-terminal [^{15}N]amide of LCTA-1421, based on earlier structural characterization of LCTA-1110 complexed to PG.[15] LCTA-1110 is a fluorinated analogue of LCTA-1421 with a *p*-fluorophenylpiperazinamide at the C-terminal position (Figure 4, top).

Structural characterization of LCTA-1110 complexed to PG provided the first clue that the C-terminus of LCTA-1110 might be involved in binding to the non-D-Ala-D-Ala segment of the PG stem structure,[15] which led to the synthesis of LCTA-1421 for investigating the interaction. Figure 4 shows the ^{13}N{^{19}F} REDOR spectra of whole cells of *S. aureus* grown in defined medium containing L-[^{15}N]Ala (left) and L-[ε-^{15}N]Lys (right) complexed with LCTA-1110 (top) during a 19.2 ms dipolar evolution.[15] The measured ^{15}N–^{19}F distance from the ^{19}F of LCTA-1110 to the L-[^{15}N]Ala of the bound PG was 6.0 Å, and the distance to the L-[ε-^{15}N]Lys was 7.9 Å.[15] REDOR distances unambiguously position the fluorine of LCTA-1110 away from the bound D-Ala-D-Ala dipeptide but near the L-Ala of the bound PG stem. Therefore, in the PG–LCTA-1421 complex, the methyl carbon of L-[3-^{13}C]Ala in the PG stem is dephased exclusively by the C-terminal [^{15}N]amide of LCTA-1421, positioning the C-terminal [^{15}N]amide close to L-[3-^{13}C]Ala. The ^{13}C{^{15}N}REDOR dephasing curve and the measured distances are shown in Figure 6.

^{15}N{^{13}C}REDOR NMR of the PG–LCTA-1421 Complex. The positioning of the C-terminal [^{15}N]amide of LCTA-1421 in the proximity of L-[3-^{13}C]Ala is confirmed in Figure 5, which shows the ^{15}N{^{13}C}REDOR spectra of whole cells of *S. aureus* grown in defined medium containing D-[1-^{13}C]Ala and L-[3-^{13}C]Ala complexed to LCTA-1421 during the 16.2 ms dipolar evolution. The inset shows the partially resolved amide peaks of LCTA-1421. The 85 ppm peak is assigned to the

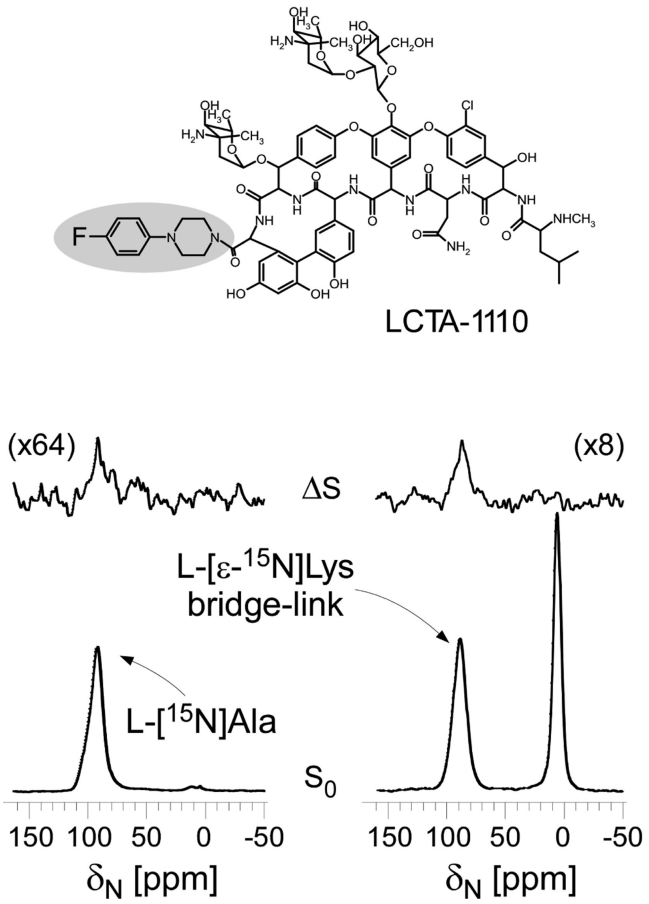

Figure 4. ^{15}N{^{19}F} REDOR spectra during 19.2 ms dipolar evolution of whole cells of *S. aureus* grown in defined medium containing L-[^{15}N]Ala (left) and L-[ε-^{15}N]Lys (right) complexed with LCTA-1110 (top). The difference spectra (Δ*S*) are on the top and the full-echo spectra (S_0) on the bottom. The ^{15}N–^{19}F distance from the L-[^{15}N]Ala of PG to the ^{19}F of LCTA-1110 is 6.0 Å, and the distance from the L-[ε-^{15}N]Lys to the ^{19}F of LCTA-1110 is 7.9 Å. The ^{15}N{^{19}F} REDOR dephasing curve can be found in ref 15.

[^{15}N]amide of the asparagine side chain and the 92 ppm peak to the C-terminal [^{15}N]amide of LCTA-1421. In the Δ*S* spectrum, the C-terminal [^{15}N]amide at 92 ppm is dephased by the ^{13}C methyl carbon of the L-[3-^{13}C]Ala and the 85 ppm peak by the ^{13}C carbonyl carbons of the bound D-[1-^{13}C]Ala-D-[1-^{13}C]Ala segment.

^{13}C–^{15}N REDOR Distance Constraints for the PG–LCTA-1421 Complex. The calculated ^{13}C{^{15}N}REDOR dephasing curves for whole cells of *S. aureus* labeled with D-[1-^{13}C]Ala and L-[3-^{13}C]Ala complexed with LCTA-1421 are shown in Figure 6 (left). The dephasing curve for the carboxyl D-[1-^{13}C]Ala_5 is shown as a red solid line, and the curve of the peptidyl carbonyl carbon of D-[1-^{13}C]Ala_4 is shown as a red dotted line. Each calculated dephasing curve includes the ^{13}C natural abundance contribution, which is fully dephased to 1% by 2 ms. The calculated ^{13}C–^{15}N distances from the Asn [^{15}N]amide of LCTA-1421 to the carboxyl and peptidyl carbonyl carbons of the bound D-[1-^{13}C]Ala-D-[1-^{13}C]Ala are 4.8 and 5.1 Å, respectively. The ^{13}C–^{15}N distance from the C-terminal [^{15}N]amide of LCTA-1421 to the alanyl methyl carbon of L-[3-^{13}C]Ala (30 ppm) is 3.5 Å. This positions the [^{15}N]amide of the asparagine side chain in LCTA-1421 3.5 Å from the L-[3-^{13}C]Ala and the C-terminal [^{15}N]amide 5.1 and

DOI: 10.1021/acs.biochem.6b00188
Biochemistry 2016, 55, 3383–3391

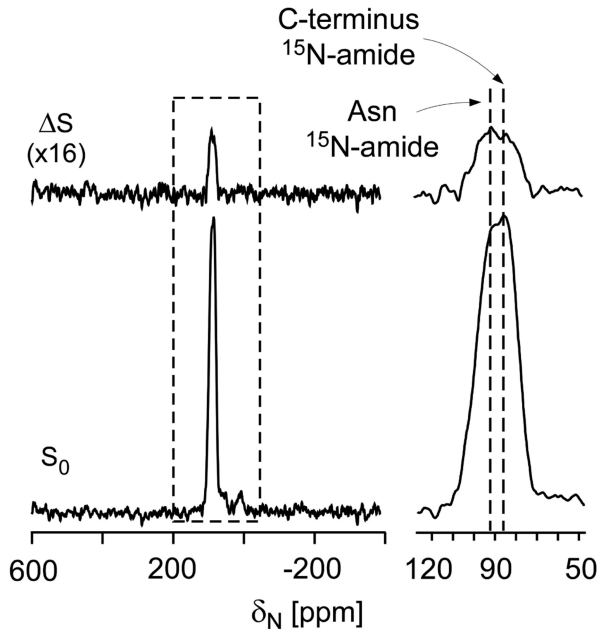

Figure 5. $^{15}N\{^{13}C\}$ REDOR spectra during the 16.2 ms dipolar evolution of whole cells of *S. aureus* grown in defined medium containing D-[1-^{13}C]Ala and L-[3-^{13}C]Ala complexed to LCTA-1421. The full-echo spectrum (S_0) is shown at the bottom and the REDOR difference spectrum (ΔS) at the top. The amide regions of the full-echo and difference spectra are inset. The [^{15}N]amide of Asn in LCTA-1421 found at 92 ppm is resolved from the [^{15}N]amide of the C-terminal amide at 85 ppm. The spectra were the result of the accumulation of 248770 scans.

4.8 Å from the ^{13}C atoms in the bound D-[1-^{13}C]Ala$_4$-D-[1-^{13}C]Ala$_5$ dipeptide, respectively.

Comparable ^{13}C−^{15}N distances are determined from ^{15}N-{^{13}C}REDOR dephasing curves shown in Figure 6 (right). The red line is the calculated dephasing curve for asparagine [^{15}N]amide dephasing (red circles) for two ^{13}C−^{15}N distances of 4.3 and 5.5 Å. The blue line is the calculated dephasing curve for the C-terminal [^{15}N]amide of LCTA-1421 dephasing (blue circles) for a ^{13}C−^{15}N distance of 3.8 Å. The ^{13}C−^{15}N distances determined by $^{15}N\{^{13}C\}$REDOR are in reasonable agreement with the $^{13}C\{^{15}N\}$REDOR results. The measured ^{13}C−^{15}N distances are illustrated in Figure 6 (bottom) and are summarized in Supplementary Table S1. The measured REDOR distances are used as constraints for the molecular dynamics simulation of LCTA-1421 complexed to the PG stem structure shown in Figure 6.

Antimicrobial Activities of the Carboxyl-Terminally Modified Glycopeptide Antibiotics. Supplementary Table S2 shows the minimal inhibitory concentrations (MICs) of vancomycin, eremomycin, LCTA-1421, and LCTA-1110 against vancomycin-susceptible and -resistant strains of Gram-positive bacteria. The C-terminally modified glycopeptides, LCTA-1421 and LCTA-1110, exhibit mild improved activities across the board against vancomycin-susceptible Gram-positive bacteria, vancomycin intermediate-resistant *S. aureus*, and vancomycin-resistant *E. faecium* and *E. faecalis*.

DISCUSSION

The LCTA-1421 Asparagine Side Chain Functions as a "Flap". Structure−activity studies have shown that the asparagine is essential for the activities in Type I glycopeptides.[2,11,22] Schäfer et al.[34] proposed that the vancomycin asparagine side chain functions as a gate to regulate access of the ligand to the binding cleft. In an "open" conformation in the X-ray crystal structure of an asymmetric vancomycin dimer, the asparagine side chain swings out of the binding cleft with an acetate ion occupying the D-Ala-D-Ala binding site. In a "closed" conformation, the asparagine side chain swings into the binding cleft.[34] An X-ray crystal structure of vancomycin bound to diacetyl-L-Lys-D-Ala-D-Ala (Figure 2, left) also showed that the asparagine side chain swings out of the binding cleft to accommodate ligand binding. Loll et al.[35] proposed that the asparagine side chain functions as a "flap" in the absence of a ligand, acting as a ligand surrogate by occupying the binding site. The "flap" prevents the hydration of the ligand binding cavity, which is energetically favorable as the water molecules placed within a highly polarized binding pocket are thought to be difficult to remove for the ligand to bind.

It is unclear how critical the "flap" is for the glycopeptide activity. As shown in Supplementary Figure S1, Type III and IV glycopeptides have aromatic residues at amino acid positions 1 and 3 that are cross-linked by a phenolic−ether linkage. This rigid macrocylic ring structure is incompatible with the proposed "flap" function in vancomycin, and furthermore, glycopeptide antibiotics of Types III and IV exhibit potent antimicrobial activities, even in the absence of the "flap", suggesting that asparagine's "flap" mechanism might not have a significant effect.

The LCTA-1421 Asparagine Side Chain Forms a Binding Cleft. REDOR measurements position the asparagine [^{15}N]amide of LCTA-1421 5.1 and 4.8 Å from the ^{13}C carbonyl carbons of D-[1-^{13}C]Ala-D-[1-^{13}C]Ala, respectively, of the bound PG stem (Figure 6). The proximity of the asparagine [^{15}N]amide to the binding cleft is contrary to the average N−C distances of 7.9 and 6.1 Å determined by X-ray diffraction on vancomycin's hexamer repeat unit (PDB entry 1FVM). Each individual N−C distance in vancomycin's hexamer unit is tabulated and shown in Supplementary Table S3. In an X-ray crystal structure, the asparagine side chain of vancomycin is positioned out of the D-Ala-D-Ala binding site; in contrast, solid-state NMR positions the asparagine side chain closer to the D-Ala-D-Ala binding pocket. We believe that the crystallization of vancomycin, forming a hexamer repeat unit, affects the conformation of the vancomycin−dipeptide structure. In comparison, solution-state NMR of the chloroeremomycin dimer determines that the corresponding N−C distances are 6.9 and 4.4 Å.[10] The solution-state NMR measurement agrees closely with REDOR NMR distance measurements of 5.1 and 4.8 Å (Figure 6). However, one caveat is that the solution NMR structure represents a chloroeremomycin bound to a model peptide mimicking PG as a dimer. We have found that glycopeptide antibiotics that readily form a dimer in solution[36−38] when complexed to whole cells of *S. aureus* are found as a monomer when bound to PG.[15,16,39] Even one of the strongest dimer-forming glycopeptides, oritavancin, is found as a monomer when complexed to the PG in whole cells of *S. aureus*.[16] Hence, distance constraints determined by REDOR NMR represent the *in vivo* glycopeptide conformation of monomeric PG binding in the cell wall of intact whole cells, without any effects from drug dimerization, PG mimic binding, or crystal lattice constraints.

We propose an alternative relationship between the asparagine side chain and the formation of the ligand binding site. The asparagine side chain does not directly form a

DOI: 10.1021/acs.biochem.6b00188
Biochemistry 2016, 55, 3383−3391

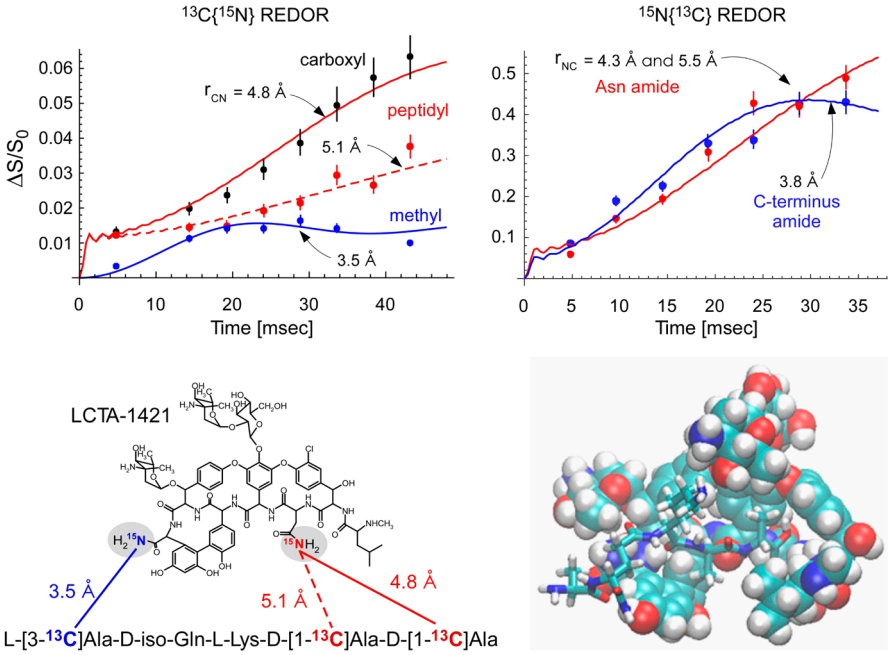

Figure 6. $^{13}C\{^{15}N\}$ REDOR dephasing (top left) for whole cells of *S. aureus* grown in defined medium containing D-[1-^{13}C]Ala and L-[3-^{13}C]Ala complexed to LCTA-1421 plotted as a function of dipolar evolution. The calculated $^{13}C\{^{15}N\}$ REDOR dephasing curves for 175 ppm (solid red line), 173 ppm (dotted red line), and 30 ppm (solid blue line) correspond to $^{13}C-^{15}N$ distances of 5.1, 4.8, and 3.5 Å, respectively. The $^{13}C\{^{15}N\}$ REDOR dephasing curve is the result of the total accumulation of 475396 scans for each S_0 and S spectrum. $^{15}N\{^{13}C\}$ REDOR dephasing (top right) plotted as a function of dipolar evolution. The red line represents the calculated $^{15}N\{^{13}C\}$ REDOR dephasing curve for $^{15}N-^{13}C$ distances of 4.3 and 5.5 Å and the distances between the asparagine [^{15}N]amide side chain and the ^{13}C atoms of D-[1-^{13}C]Ala-D-[1-^{13}C]Ala bound to LCTA-1421. The blue line represents the dephasing curve for the $^{15}N-^{13}C$ distance of 3.8 Å between the C-terminal [^{15}N]amide of LCTA-1421 and the ^{13}C of L-[3-^{13}C]Ala of PG. The $^{15}N\{^{13}C\}$ REDOR dephasing curve is result of the total accumulation of 1036810 scans. Summary (bottom left) of measured REDOR distance constraints. Molecular dynamics simulation model structure (bottom right) of LCTA-1421 bound to a pentapeptide PG stem structure (L-Ala-D-iso-Gln-L-Lys-D-Ala-D-Ala). The simulation was conducted without water molecules with the following solid-state NMR distance constraints: (i) 3.5 Å between L-[3-^{13}C]Ala and a [^{15}N]amide at the C-terminus of LCTA-1421, (ii) 5.1 Å between D-[1-^{13}C]Ala and the asparagine [^{15}N]amide in LCTA-1421, and (iii) 4.8 Å between D-[1-^{13}C]Ala and the [^{15}N]amide at the C-terminus of LCTA-1421. REDOR NMR measurement of the complex of LCTA-1241 with whole cell *S. aureus* places the [^{15}N]amide side chain of asparagine approximately 5 Å from the carbonyl carbons of the bound D-Ala-D-Ala of PG. This is contrary to the position of the asparagine side chain found outside of the D-Ala-D-Ala binding pocket in X-ray crystal structures.

hydrogen bond with D-Ala-D-Ala, but its proximity to the bound dipeptide strongly suggests a possible interaction with the *N*-methylleucine (first amino acid of LCTA-1421). The interaction of the asparagine side chain with the *N*-methylleucine can form a binding cavity that can stabilize dipeptide binding. Either Edman degradation of the *N*-methylleucine in eremomycin (the parent compound of LCTA-1421)[40] or the replacement of asparagine with glutamine or aspartate can disrupt this action, thus decreasing antimicrobial activities. In the case of substitution of asparagine with isoaspartate, the D-Ala-D-Ala binding site is destroyed by rearrangement, forming CDP-I, which is devoid of antimicrobial activities.[41] REDOR distance constraints indicate that the asparagine and leucine side chains constitute a part of a hydrophobic pocket necessary for D-Ala-D-Ala binding. The proposed interaction between the asparagine and *N*-methylleucine in the presence of dipeptide will require further investigation.

The Carboxyl Terminus of LCTA-1421 Interacts with the Non-D-Ala-D-Ala Segments of PG. The solid-state NMR measurements position the L-Ala segment of the bound PG stem near the C-terminus of LCTA-1421 (Figure 6). The measured $^{13}C-^{15}N$ distance between the C-terminal [^{15}N]amide of LCTA-1421 and the L-[3-^{13}C]Ala of the PG stem is 3.5 Å as determined by $^{13}C\{^{15}N\}$ REDOR (Figure 3) and 3.8 Å as determined by $^{15}N\{^{13}C\}$REDOR (Figure 5). The results are in excellent agreement with the position of fluorine in LCTA-1110 (Figure 4) bound to PG in intact whole cells of *S. aureus* determined at 6.0 Å from the ^{15}N of L-[^{15}N]Ala of the bound PG stem.[32] These structural measurements are consistent with the C-terminus of glycopeptide interacting with the non-D-Ala-D-Ala segments of PG.

The MIC measurements (Supplementary Table S2) show that the C-terminal modifications enhance the antimicrobial activities of glycopeptides. The MIC values of LCTA-1421 and LCTA-1110 are greater than those of the parent compound eremomycin. The activities are enhanced because the C-terminal modification enhances glycopeptide–PG binding through interactions that involve more than just D-Ala-D-Ala binding. REDOR distance constraints position the C-terminus of LCTA-1421 in the vicinity of the L-Ala of the bound PG stem structure in intact whole cells of *S. aureus*. This non-D-Ala-D-Ala interaction is critical for permitting the binding of the drug to the D-Ala-D-Lac-terminated PG stem found in vancomycin-resistant enterococci and thus is likely to be responsible for the small enhancement in the activity of LCTA-1421 against vancomycin-resistant and intermediate-resistant pathogens (Supplementary Table S2).

In conclusion, glycopeptide antibiotics exhibit potent antibacterial activities by inhibiting PG biosynthesis in Gram-

DOI: 10.1021/acs.biochem.6b00188
Biochemistry 2016, 55, 3383–3391

positive bacteria. The primary glycopeptide−PG interaction involves the aglycon structure of the glycopeptide binding to the D-Ala-D-Ala of the PG stem structure. However, structure−activity relationship studies of chemically modified glycopeptides suggest that drug−target interaction is complex. In the case of C-terminally modified glycopeptides, the antibiotic C-terminal interactions with the non-D-Ala-D-Ala segments of PG improve drug activity. To investigate interactions of glycopeptides with non-D-Ala-D-Ala segments of PG, we complexed LCTA-1421 to intact whole cells of *S. aureus* and characterized the PG−LCTA-1421 complex using solid-state NMR. We have synthesized LCTA-1421 for this study with selective incorporations of the ^{15}N isotope into its aglycon structure, one at the Asn side chain and the other at the C-terminus. REDOR NMR measurements positioned the [^{15}N]amide of the Asn side chain of LCTA-1421 is the proximity (5.1 and 4.8 Å) of the ^{13}C atoms in the bound D-[1-^{13}C]Ala-D-[1-^{13}C]Ala dipeptide, which indicated that the asparagine plays an important role in D-Ala-D-Ala binding. We have also found that the C-terminal [^{15}N]amide of LCTA-1421 is positioned in the proximity of the L-[1-^{13}C]Ala segment of the bound PG stem. Future experiments will be required to further investigate the interactions of the C-terminus of the glycopeptide with the non-D-Ala-D-Ala segment of the PG stem structure, which is crucial for enhancing antimicrobial activity against the vancomycin-resistant enterococci. Multiple REDOR distance constraints will be used to develop a detailed molecular model structure of the glycopeptide−PG complex to provide structural insight for the development of novel therapeutic agents against emerging multidrug-resistant pathogens.

■ ASSOCIATED CONTENT

Supporting Information

The Supporting Information is available free of charge on the ACS Publications website at DOI: 10.1021/acs.biochem.6b00188.

Chemical structures of classes of glycopeptide antibiotics, a summary table of $^{13}C-^{15}N$ REDOR distance constraints determined for LCTA-1421 bound to peptidoglycan in intact whole cells of *S. aureus*, and minimal inhibitory concentrations of C-terminally modified glycopeptide antibiotics against vancomycin-susceptible and -resistant pathogens (PDF)

■ AUTHOR INFORMATION

Corresponding Author

*E-mail: Sung_J_Kim@baylor.edu.

Funding

This paper is based on work supported by National Institutes of Health Grant GM116130.

Notes

The authors declare no competing financial interest.

■ ACKNOWLEDGMENTS

The authors acknowledge Southern Methodist University's Center for Scientific Computation for computing resources and thank Ms. Svetlana E. Solovieva and Ms. Elena P. Mirchink, D.Sc. (Gause Institute of New Antibiotics), for the antibacterial activity of LCTA compounds.

■ ABBREVIATIONS

$^{13}C\{^{15}N\}$, carbon channel observation with nitrogen dephasing; VRE, vancomycin-resistant enterococci; VSE, vancomycin-susceptible enterococci; HBPyU, (benzotriazol-1-yloxy)-dipyrrolidinocarbenium hexafluorophosphate; LCTA-1421, bis-[^{15}N]amide-carboxyeremomycin; LCTA-1110, eremomycin *p*-fluorophenylpiperazinamide; $^{15}N\{^{13}C\}$, nitrogen channel observation with carbon dephasing; PG, peptidoglycan; CPMAS, cross-polarization at magic-angle spinning; lipid II, *N*-acetylglucosamine-*N*-acetyl-muramyl-pentapeptide-pyrophosphoryl-undecaprenol; REDOR, rotational-echo double-resonance; PyBOP, (benzotriazol-1-yloxy)-tripyrrolidinophosphonium hexafluorophosphate; PDB, Protein Data Bank.

■ REFERENCES

(1) Goff, D. (2002) Antimicrobial Efficacy Review. *Infectious Disease Special Edition 5*, 31−34.

(2) Nagarajan, R. (1994) *Glycopeptide Antibiotics*, Vol. *63*, Marcel Dekker, New York.

(3) Nicolaou, K. C., Cho, S. Y., Hughes, R., Winssinger, N., Smethurst, C., Labischinski, H., and Endermann, R. (2001) Solid- and solution-phase synthesis of vancomycin and vancomycin analogues with activity against vancomycin-resistant bacteria. *Chem. - Eur. J. 7*, 3798−3823.

(4) Loll, P. J., and Axelsen, P. H. (2000) The structural biology of molecular recognition by vancomycin [In Process Citation]. *Annu. Rev. Biophys. Biomol. Struct. 29*, 265−289.

(5) Matsuhashi, M., Dietrich, C. P., and Strominger, J. L. (1965) Incorporation of glycine into the cell wall glycopeptide in *Staphylococcus aureus*: role of sRNA and lipid intermediates. *Proc. Natl. Acad. Sci. U. S. A. 54*, 587−594.

(6) Cegelski, L., Kim, S. J., Hing, A. W., Studelska, D. R., O'Connor, R. D., Mehta, A. K., and Schaefer, J. (2002) Rotational-echo double resonance characterization of the effects of vancomycin on cell wall synthesis in *Staphylococcus aureus*. *Biochemistry 41*, 13053−13058.

(7) Hammes, W. P., and Neuhaus, F. C. (1974) On the mechanism of action of vancomycin: inhibition of peptidoglycan synthesis in Gaffkya homari. *Antimicrob. Agents Chemother. 6*, 722−728.

(8) Rao, J., Colton, I. J., and Whitesides, G. M. (1997) Using Capillary Electrophoresis To Study the Electrostatic Interation Involved in the Association of D-Ala-D-Ala with Vancomycin. *J. Am. Chem. Soc. 119*, 9336−9340.

(9) Nitanai, Y., Kikuchi, T., Kakoi, K., Hanamaki, S., Fujisawa, I., and Aoki, K. (2009) Crystal structures of the complexes between vancomycin and cell-wall precursor analogs. *J. Mol. Biol. 385*, 1422−1432.

(10) Prowse, W. G., Kline, A. D., Skelton, M. A., and Loncharich, R. J. (1995) Conformation of A82846B, a glycopeptide antibiotic, complexed with its cell wall fragment: an asymmetric homodimer determined using NMR spectroscopy. *Biochemistry 34*, 9632−9644.

(11) Nagarajan, R. (1993) Structure-activity relationships of vancomycin-type glycopeptide antibiotics. *J. Antibiot. 46*, 1181−1195.

(12) Kim, S. J., Singh, M., and Schaefer, J. (2009) Oritavancin binds to isolated protoplast membranes but not intact protoplasts of *Staphylococcus aureus*. *J. Mol. Biol. 391*, 414−425.

(13) Kim, S. J., and Schaefer, J. (2008) Hydrophobic side-chain length determines activity and conformational heterogeneity of a vancomycin derivative bound to the cell wall of *Staphylococcus aureus*. *Biochemistry 47*, 10155−10161.

(14) Kim, S. J., Matsuoka, S., Patti, G. J., and Schaefer, J. (2008) Vancomycin derivative with damaged D-Ala-D-Ala binding cleft binds to cross-linked peptidoglycan in the cell wall of *Staphylococcus aureus*. *Biochemistry 47*, 3822−3831.

(15) Kim, S. J., Cegelski, L., Preobrazhenskaya, M., and Schaefer, J. (2006) Structures of *Staphylococcus aureus* cell-wall complexes with vancomycin, eremomycin, and chloroeremomycin derivatives by ^{13}C-

DOI: 10.1021/acs.biochem.6b00188
Biochemistry 2016, 55, 3383−3391

{^{19}F} and ^{15}N{^{19}F} rotational-echo double resonance. *Biochemistry 45*, 5235−5250.
(16) Kim, S. J., Cegelski, L., Studelska, D. R., O'Connor, R. D., Mehta, A. K., and Schaefer, J. (2002) Rotational-echo double resonance characterization of vancomycin binding sites in *Staphylococcus aureus*. *Biochemistry 41*, 6967−6977.
(17) Olsufyeya, E. N., Berdnikova, T. F., Miroshnikova, O. V., Reznikova, M. I., and Preobrazhenskaya, M. N. (1999) Chemical modification of antibiotic eremomycin at the asparagine side chain. *J. Antibiot. 52*, 319−324.
(18) Cooper, R. D., Snyder, N. J., Zweifel, M. J., Staszak, M. A., Wilkie, S. C., Nicas, T. I., Mullen, D. L., Butler, T. F., Rodriguez, M. J., Huff, B. E., and Thompson, R. C. (1996) Reductive alkylation of glycopeptide antibiotics: synthesis and antibacterial activity. *J. Antibiot. 49*, 575−581.
(19) Nicas, T. I., Mullen, D. L., Flokowitsch, J. E., Preston, D. A., Snyder, N. J., Zweifel, M. J., Wilkie, S. C., Rodriguez, M. J., Thompson, R. C., and Cooper, R. D. (1996) Semisynthetic glycopeptide antibiotics derived from LY264826 active against vancomycin-resistant enterococci. *Antimicrob. Agents Chemother. 40*, 2194−2199.
(20) Malabarba, A., Nicas, T. I., and Thompson, R. C. (1997) Structural modifications of glycopeptide antibiotics. *Med. Res. Rev. 17*, 69−137.
(21) Rodriguez, M. J., Snyder, N. J., Zweifel, M. J., Wilkie, S. C., Stack, D. R., Cooper, R. D., Nicas, T. I., Mullen, D. L., Butler, T. F., and Thompson, R. C. (1998) Novel glycopeptide antibiotics: N-alkylated derivatives active against vancomycin-resistant enterococci. *J. Antibiot. 51*, 560−569.
(22) Miroshnikova, O. V., Printsevskaya, S. S., Olsufyeva, E. N., Pavlov, A. Y., Nilius, A., Hensey-Rudloff, D., and Preobrazhenskaya, M. N. (2000) Structure-activity relationships in the series of eremomycin carboxamides. *J. Antibiot. 53*, 286−293.
(23) Gullion, T., and Schaefer, J. (1989) Detection of weak heteronuclear dipolar coupling by rotational-echo double-resonance nuclear magnetic resonance. *Adv. Magn. Opt. Reson. 13*, 57−83.
(24) Gullion, T., and Schaefer, J. (1989) Rotational-echo double-resonance NMR. *J. Magn. Reson. 81*, 196−200.
(25) Solov'eva, S. E., Printsevskaya, S. S., Olsuf'eva, E. N., Batta, G., and Preobrazhenskaya, M. N. (2008) New derivatives of eremomycin containing ^{15}N or F atoms for NMR study. *Russ. J. Bioorg. Chem. 34*, 747−754.
(26) Kim, S. J., Preobrazhenskaya, M., and Schaefer, J. (2008) Characterization of *Staphylococcus aureus* peptidoglycan tertiary structure using glycopeptides as probe by solid-state NMR. Interscience Conference on Antimicrobial Agents and Chemotherapy, Washington, DC, F2-2073.
(27) Tong, G., Pan, Y., Dong, H., Pryor, R., Wilson, G. E., and Schaefer, J. (1997) Structure and dynamics of pentaglycyl bridges in the cell walls of *Staphylococcus aureus* by ^{13}C-^{15}N REDOR NMR. *Biochemistry 36*, 9859−9866.
(28) Gullion, T., Baker, D. B., and Conradi, M. S. (1990) New, compensated Carr-Purcell sequences. *J. Magn. Reson. 89*, 479−484.
(29) Mueller, K. T., Jarvie, T. P., Aurentz, D. J., and Roberts, B. W. (1995) The REDOR transform: direct calculation of internuclear couplings from dipolar-dephasing NMR data. *Chem. Phys. Lett. 242*, 535−542.
(30) d'Espinose de la Caillerie, J.-B., and Fretigny, C. (1998) Analysis of the REDOR signal and inversion. *J. Magn. Reson. 133*, 273−280.
(31) Vanommeslaeghe, K., and MacKerell, A. D., Jr. (2012) Automation of the CHARMM General Force Field (CGenFF) I: bond perception and atom typing. *J. Chem. Inf. Model. 52*, 3144−3154.
(32) Kim, S. J., Singh, M., Preobrazhenskaya, M., and Schaefer, J. (2013) Staphylococcus aureus peptidoglycan stem packing by rotational-echo double resonance NMR spectroscopy. *Biochemistry 52*, 3651−3659.
(33) Cegelski, L., Steuber, D., Mehta, A. K., Kulp, D. W., Axelsen, P. H., and Schaefer, J. (2006) Conformational and quantitative characterization of oritavancin-peptidoglycan complexes in whole cells of *Staphylococcus aureus* by in vivo ^{13}C and ^{15}N labeling. *J. Mol. Biol. 357*, 1253−1262.
(34) Schäfer, M., Schneider, T. R., and Sheldrick, G. M. (1996) Crystal structure of vancomycin. *Structure 4*, 1509−1515.
(35) Loll, P. J., Bevivino, A. E., Korty, B. D., and Axelsen, P. H. (1997) Simultaneous recognition of a carboxylate-containing ligand and an intramolecular aurrogate ligand in the crystal structure of an asymmetric vancomycin dimer. *J. Am. Chem. Soc. 119*, 1516−1522.
(36) Sharman, G. J., Try, A. C., Dancer, R. J., Cho, Y. R., Staroske, T., Bardsley, B., Maguire, A. J., Cooper, M. A., O'Brien, D. P., and Williams, D. H. (1997) The roles of dimerization and membrane anchoring in activity of glycopeptide antibiotics against vancomycin-resistant bacteria. *J. Am. Chem. Soc. 119*, 12041−12047.
(37) Allen, N. E., LeTourneau, D. L., and Hobbs, J. N., Jr. (1997) The role of hydrophobic side chains as determinants of antibacterial activity of semisynthetic glycopeptide antibiotics. *J. Antibiot. 50*, 677−684.
(38) Beauregard, D. A., Williams, D. H., Gwynn, M. N., and Knowles, D. J. (1995) Dimerization and membrane anchors in extracellular targeting of vancomycin group antibiotics. *Antimicrob. Agents Chemother. 39*, 781−785.
(39) Kim, S. J., Tanaka, K. S., Dietrich, E., Rafai Far, A., and Schaefer, J. (2013) Locations of the hydrophobic side chains of lipoglycopeptides bound to the peptidoglycan of *Staphylococcus aureus*. *Biochemistry 52*, 3405−3414.
(40) Printsevskaya, S. S., Pavlov, A. Y., Olsufyeva, E. N., Mirchink, E. P., Isakova, E. B., Reznikova, M. I., Goldman, R. C., Branstrom, A. A., Baizman, E. R., Longley, C. B., Sztaricskai, F., Batta, G., and Preobrazhenskaya, M. N. (2002) Synthesis and mode of action of hydrophobic derivatives of the glycopeptide antibiotic eremomycin and des-(N-methyl-D-leucyl)eremomycin against glycopeptide-sensitive and -resistant bacteria. *J. Med. Chem. 45*, 1340−1347.
(41) Harris, C. M., Kopecka, H., and Harris, T. M. (1985) The stabilization of vancomycin by peptidoglycan analogs. *J. Antibiot. 38*, 51−57.
(42) Nitanai, Y., Kakoi, K., and Aoki, K. (2000) Crystal Structure of the Complex between Vancomycin and a Cell wall Precursor Analog, Di-Acetyl-Lys-D-Ala-D-Ala. Protein Data Bank.

DOI: 10.1021/acs.biochem.6b00188
Biochemistry 2016, 55, 3383−3391